

---

# Stabilizing Oxygen Lattice and Reversible Oxygen Redox Chemistry through Structural Dimensionality in Li-rich Cathode Oxides

Enyue Zhao<sup>+</sup>, Qinghao Li<sup>+</sup>, Fanqi Meng<sup>+</sup>, Jue Liu, Junyang Wang, Lunhua He, Zheng Jiang, Qinghua Zhang, Xiqian Yu<sup>\*</sup>, Lin Gu<sup>\*</sup>, Wanli Yang<sup>\*</sup>, Hong Li, Fangwei Wang<sup>\*</sup> and Xuejie Huang

---

[\*] E. Zhao, Dr. Q. Li, F. Meng, J. Wang, Prof. L. He, Dr. Q. Zhang, Prof. X. Yu<sup>\*</sup>, Prof. L. Gu<sup>\*</sup>, Prof. H. Li, Prof. F. Wang<sup>\*</sup>, Prof. X. Huang,  
Institute of Physics  
Chinese Academy of Sciences  
Beijing 100190, China  
University of Chinese Academy of Sciences  
Beijing 100049, China  
Songshan Lake Materials Laboratory  
Dongguan, Guangdong 523808, China  
E-mail: xyu@iphy.ac.cn, l.gu@iphy.ac.cn, fwwang@iphy.ac.cn  
Dr. W. Yang<sup>\*</sup>  
Advanced Light Source  
Lawrence Berkeley National Laboratory  
Berkeley, CA 94720, USA  
E-mail: WLYang@lbl.gov  
Dr. J. Liu  
Neutron Scattering Division  
Oak Ridge National Laboratory  
Oak Ridge, TN 37831, USA  
Dr. J. Zheng  
Shanghai Synchrotron Radiation Facility  
Shanghai, 201204, China

[<sup>+</sup>] These authors contributed equally to this work.

Supporting information for this article is given via a link at the end of the document.

---

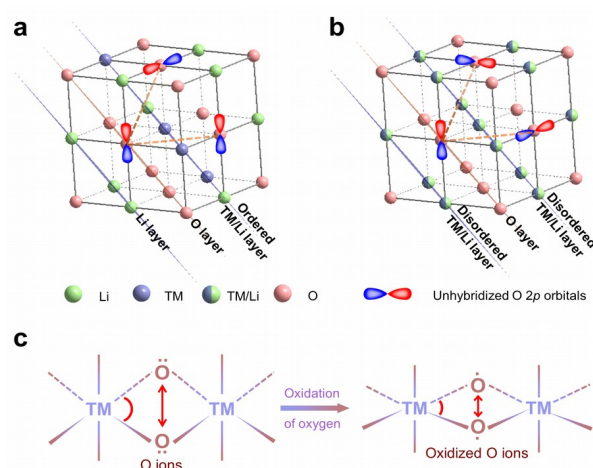
**Abstract:** Lattice oxygen redox (I-OR) has become an essential complementation for the traditional transition-metal (TM) redox charge compensation to achieve the high capacity in Li-rich cathode oxides. However, the understanding of I-OR chemistry remains elusive, and a critical question is the structural effect on the stability of I-OR reactions. Herein, the coupling between I-OR and structure dimensionality is researched. We reveal that the oxygen lattice structure evolution upon the I-OR in Li-rich TM oxides with tridimensional (3D)-disordered cation framework is relatively stable, directly contrasting the obviously distorted oxygen lattice framework in Li-rich oxides with two-dimensional (2D)/3D-ordered cation structure. Our results highlight the role of structure dimensionality in stabilizing oxygen lattice involving reversible I-OR, which broadens the horizon for designing high-energy-density Li-rich cathode oxides with stable I-OR chemistry.

Due to the attainable ultrahigh capacity, Li-rich transition-metal (TM) oxides have attracted wide attention as the cathode candidates for high-energy-density Li-ion batteries.<sup>[1]</sup> It has been reported that the anomalously high capacity in these materials originates from the cumulative redox of TMs and lattice oxygen.<sup>[2]</sup> Unlike the TM redox chemistry, the lattice oxygen redox (I-OR) is more intricate and its mechanistic understanding is yet to be clarified. Additionally, it seems that the oxygen redox activities may cause detrimental effects (e.g., irreversible structure transition) on the electrochemical performance.<sup>[3]</sup> At this time, in-depth characterizations of the I-OR chemistry as well as guidelines for achieving its stable operation are urgent and significant.

In Li-rich cathode oxides, a Li-O-Li coordination with unhybridized O 2p orbital was proposed to be responsible for its I-OR activity.<sup>[4]</sup> Thus, the I-OR behavior is closely associated with the spatial distribution and orientation (which is directly correlated with the structure dimensionality) of the Li-O-Li coordination (unhybridized O 2p orbital) in the overall structure.<sup>[4]</sup> For example, in Li-rich layered oxides, the unhybridized O 2p orbitals orderly distribute in the structure framework due to their 2D-ordered (e.g., honeycomb structure) TM/Li layer (Scheme 1a, Scheme S1). Literature has reported that the I-OR in these materials can be controlled by introducing stacking faults which can obviously alter the structure dimensionality along the vertical direction of TM/Li layer and thus affect the configuration of unhybridized O 2p orbitals.<sup>[5]</sup> Furthermore, the discrepant I-OR chemistry behavior was also detected in the case of Li-rich layered oxides with 3D-ordered TM/Li framework.<sup>[6]</sup> It is obvious that the structural dimensionality will affect the I-OR and define the electrochemical performance.

Nevertheless, till now, how the structure dimensionality affects the I-OR and how to employ such an effect to design a better Li-rich cathode oxide with

stable I-OR remain open questions. Therefore, it is imperative to study the I-OR in Li-rich cathode oxides with a structural dimensionality different from Li-rich layered compounds. For such a comparative study, the cation-disordered Li-rich oxides with a 3D-disordered cationic framework (Scheme 1b) becomes a perfect candidate.<sup>[7]</sup> Here, The coupling relationship between I-OR and structure dimension was revealed in cation-disordered Li-rich oxide  $\text{Li}_{1.2}\text{Ti}_{0.35}\text{Ni}_{0.35}\text{Nb}_{0.1}\text{O}_{1.8}\text{F}_{0.2}$  (LTNNbOF). Our results suggest that the structure dimensionality can be utilized effectively to design high-performance cathode oxides with stable I-OR.



**Scheme 1.** (a) 2D-ordered cation layer for Li-rich TM oxides with coplanar unhybridized O 2p orbitals in the interlayer; (b) 3D-disordered cation framework for Li-rich TM oxides with randomly spatial-distribution correlation among unhybridized O 2p orbitals; (c) Schematic for the shrink of O-O pairs distance and corresponding structure distortion.

Pure-phase LTNNbOF (Figure S1, S2) was prepared by a solid-state calcination method. Refinement results of the neutron powder diffraction (NPD) pattern confirmed its (S.G.) Fm-3m cation-disordered rock-salt structure (Figure 1a, Table S1), which can be simply described as that all the cations (TM/Li) distribute randomly in the anionic 3D-framework with the oxygen octahedron configuration (inset in Figure 1a). The nearest-neighbor TM-O (e.g., Ni-O) pairs distance ( $\sim 2.08 \text{ \AA}$ ) and O-O pairs distance ( $\sim 2.94 \text{ \AA}$ ) are refined from the local neutron pair distribution function (nPDF) patterns (Figure 1b, Table S2).

The electrochemical performance of LTNNbOF is shown in Figure 1c, in which an initial charge capacity of  $\sim 300 \text{ mA h/g}$  (equivalent to  $\sim 0.97 \text{ Li}$  extraction) and a high reversible discharge capacity of  $\sim 277 \text{ mA h/g}$  (corresponding to  $\sim 0.91 \text{ Li}$  re-insertion) were obtained. Considering the theoretical capacity of  $\sim 214 \text{ mA h/g}$  based on the  $\text{Ni}^{2+}/\text{Ni}^{4+}$  redox couple as well as the electrochemical inertness of  $\text{Ti}^{4+}$ ,  $\text{Nb}^{5+}$ ,  $\text{F}^-$  ions, I-OR needs to be naturally invoked for the charge

compensation mechanism, which is experimentally clarified below through soft X-ray absorption spectroscopy (sXAS) and mapping of resonant inelastic X-ray scattering (mRIXS).

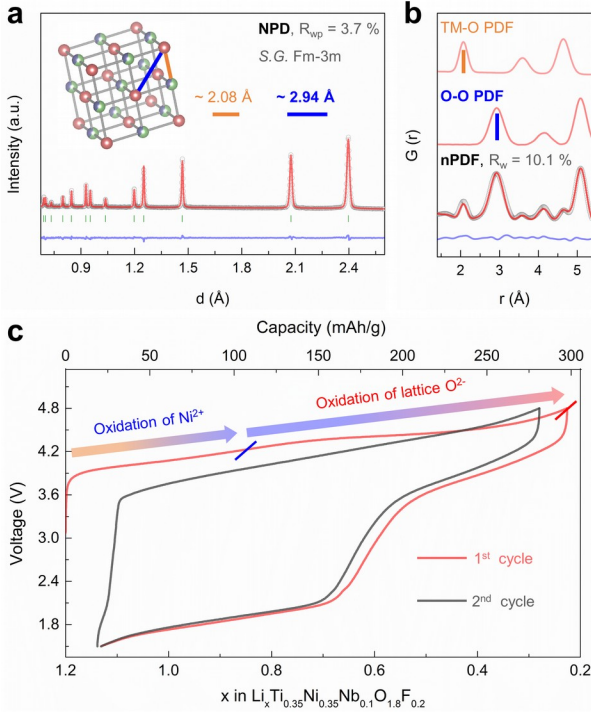


**Figure 1.** Refinement results of the (a) NPD and (b) nPDF patterns. Inset in (a) shows the crystal structure of LTNNbOF, the atomic pairs distances with corresponding PDF peaks are labeled in (b); (c) The voltage profiles of the first two cycles for LTNNbOF at 20 mA/g. See also Figure S3, 4.

TM L-edges directly probe the 3d valence states through excitations of 2p electrons to 3d orbitals, which provides the sensitivity to quantitatively determine the TM oxidation states.<sup>[8]</sup> As shown in Figure 2b and c,

partial  $\text{Ni}^{2+}$  ions were oxidized to  $\text{Ni}^{3+}$  and  $\text{Ni}^{4+}$  ions upon charging up to 4.3 V, and during the subsequent charging process, the oxidation states of Ni ions remains relatively stable. For the F,  $\text{Ti}^{4+}$  and  $\text{Nb}^{5+}$  ions, there is no observable evidence that they participate in the charge compensation (Figure S6-8).<sup>[9]</sup> This quantitative analysis indicates that the charge compensation in LTNNbOF is mainly from I-OR during charging from 4.3 V to 4.8 V.

Direct evidence of the I-OR in LTNNbOF could be revealed through oxygen spectroscopy. First, the pre-edge features of sXAS changes in lineshape and enhances in intensity upon charging (Figure S9). However, these evolutions are due to the changes in TM states and TM-O hybridization strength.<sup>[8a]</sup> Second, compared with the pristine state (Figure 2d), O-K mRIXS of the the 4.8 V charged electrode shows enhanced intensity at 523.7 eV emission and 531 eV excitation energies (white arrow in Figure 2e). It has been established that an enhanced mRIXS feature here is a signature of partially occupied O-2p bands in non-divalent oxygen, i.e., oxidized oxygen,<sup>[10]</sup> thus providing a reliable fingerprint of I-OR states in charged electrodes.<sup>[8a]</sup> Indeed, Figure 2f shows the integrated mRIXS intensity around 531 eV excitation energy, which displays a gradual enhancement of the intensity at 523.7 eV (shaded range) during charging, indicating oxidized oxygen in the charged electrodes at high potentials. Note that well isolated I-OR mRIXS feature has been found in various charged electrodes including Li-rich layered oxides,<sup>[8a]</sup> but charged LTNNbOF displays only an enhanced shoulder feature here. This is mainly due to the overlapping of I-OR and Ti-O hybridization features at exactly the same excitation energy at 531 eV, leading to only a shoulder, instead of an isolated feature, of the I-OR signals in LTNNbOF. Nonetheless, the systematic evolution of the 523.7 eV shoulder in Figure 2f upon cycling reveals the I-OR reactions in LTNNbOF, and more importantly, the intensity drops in the following discharging, indicating a reversible I-OR activity.

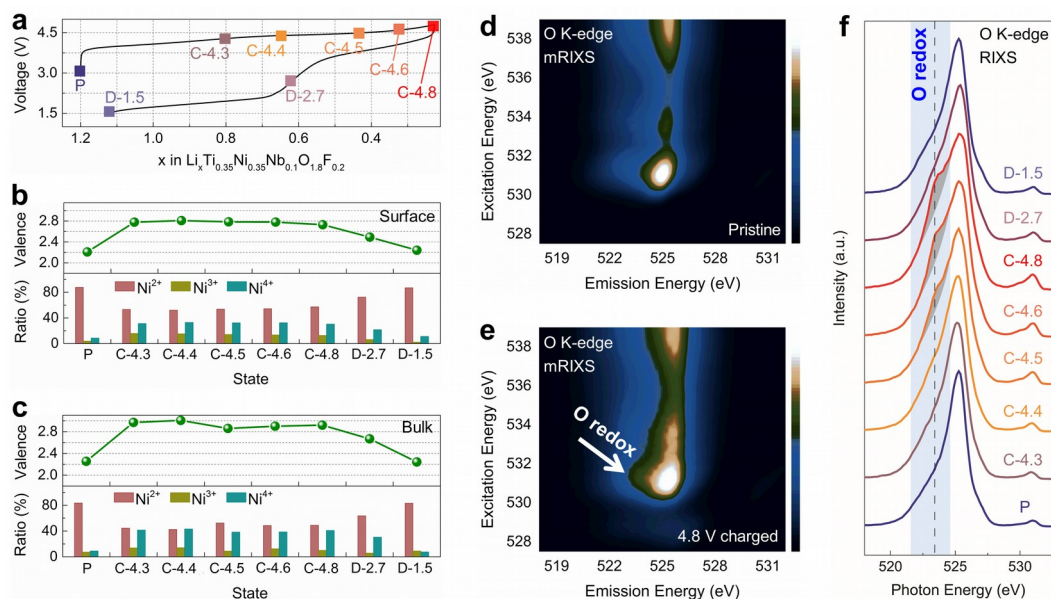


**Figure 2.** (a) The initial electrochemical cycle curve at 20 mA/g; (b) Surface and (c) bulk valence evolution of Ni ions (top panel) as well as the ratio variation of the different-valence Ni ions (bottom panel) based on the fitted Ni L-edge sXAS spectra in Figure S5; The mRIXS results of the (d) pristine and (e) 4.8 V charged electrodes; (f) The *ex situ* RIXS spectra on the O K-edge. See also scheme S2.

It has been reported that the storage of charge (or electron) on the lattice oxygen ions can alter their electronic structure, which will further affect the oxygen lattice framework (i.e., O-O atomic-pair distance).<sup>[4]</sup> Thus, nPDF, capable of highlighting the oxygen scattering and analyzing the atomic-pair coordination, was employed to directly reveal the variation of O-O pair distance in the bulk structure of LTNNbOF upon Li de/re-intercalation process. Surprisingly, no obvious change of the average O-O pair distance in LTNNbOF was observed during the electrochemical cycling (Figure 3a and Figure S10). The broad PDF peaks upon cycling may be correlated with the local variation of cations content and also due to the resolution of the diffractometer, and more accurately quantitative analysis will be done using higher-resolution instrument. The relative stable oxygen lattice was further verified by atomic-resolution scanning transmission electron microscopy (STEM) which can clearly present the projection of oxygen columns along the [110] axis without overlapping with the columns of TM or Li in LTNNbOF (Figure 3b, c). High-angle annular dark field (HAADF) STEM images in Figure 3b, c shows the almost invariant average distance among the oxygen columns projected along the [110] axis from the pristine to high-charged state. The phenomenon observed in cation-disordered Li-rich oxides with 3D-disordered cation framework is very different from the distorted TM-O octahedron with significantly shortened O-O pair distance detected in Li-rich oxides with either 2D-ordered cation layer or 3D-ordered cation framework.<sup>[2d, 6]</sup>

The contrast on the oxygen lattice stability in these Li-rich oxides could be understood by considering their

different dimensional configurations and unhybridized O 2p orbital configurations (or orientation). The electronic storage (or the production of electronic holes) usually occur on the lattice O<sup>2-</sup> ions with Li-O-Li coordination upon I-OR. To reduce the energy of the oxidized O<sup>2-</sup> ions (denoted as O<sup>-</sup>), the interaction between two O<sup>-</sup> is enhanced by decreasing the O-O pair distance, which will result in the decrease of O-TM-O angle and overlap between TM e<sub>g</sub> orbitals and O 2p orbitals. This weakens the TM-O bonding and is not favorable for the stabilization of the structure framework (Scheme 1c). In the meantime, the decrease of O-O pair distance is closely associated with the directional-distribution correlation between two unhybridized O 2p orbitals. The O-O pair distance would not obviously decrease if the two unhybridized O 2p orbitals are non-coplanar, because there is insufficiently interaction or bonding trend between them. The O-O pair distance would significantly decrease only when the corresponding unhybridized O 2p orbitals are coplanar.

For Li-rich cathode oxides with 2D-ordered cation layer, there are coplanar unhybridized O 2p orbitals in the TM interlayer (Scheme 1a) and non-coplanar unhybridized O 2p orbitals in the TM intralayer (Scheme S1) due to the ordered spatial distribution of cations. In the oxidized state, the O<sup>-</sup>-O<sup>-</sup> pairs with coplanar unhybridized O 2p orbitals would shorten their distance to reduce the energy. In contrast, for Li-rich cathode oxides with 3D-disordered cation framework (Scheme 1b), the spatial correlation between two unhybridized O 2p orbitals is disordered (random), which greatly reduce the formation probability of coplanar unhybridized O 2p orbitals. This situation makes the coplanar unhybridized

O  $2p$  orbitals, if any, randomly distribute in the structure framework. In this case, the original O-TM-O bonding-structure framework is more likely to be maintained, rather than obviously distorted during the I-OR process. Thus, no observable variation of the average O-O pair distance was found in LTNNbOF with such a 3D-disordered cation framework. (Figure 3, Figure S10-11) We note that a relatively well-preserved oxygen lattice framework is important to stabilize the reversible I-OR against other irreversible oxygen activities upon electrochemical operations.

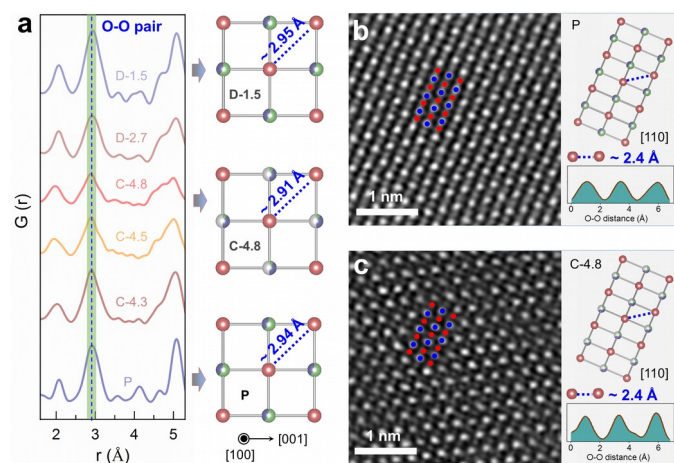


**Figure 3.** (a) The *ex situ* local nPDF patterns (left panel), and variation of the average O-O pairs distance (right panel); [110] STEM-HAADF images of the (b) pristine and (c) 4.8 V charged samples, the corresponding average distances of the nearest-neighbor O-O columns projected along the [110] axis are labeled in the structure schematic.

The finding of relatively stable oxygen lattice structure framework in the 3D-disordered LTNNbOF system, contrasting that in Li-rich layered systems, suggests that dimensional configurations could be utilized to achieve both reversible I-OR and stable structure upon electrochemical cycling. Usually, the structure transition (e.g., distortion of TM-O octahedron, gliding of TM layer, TM migration) in Li-rich cathode oxides with 2D-ordered structure is common upon I-OR, and this transition behavior would be irreversible once there is the loss of O<sub>2</sub> gas.<sup>[11]</sup> The irreversible structure transition may further induce the unstable I-OR, leading to detrimental effects in electrochemical performance (e.g., voltage fade, capacity degradation).<sup>[12]</sup> Such effects do not take place 3D-disordered structure because of its relatively robust oxygen lattice structure framework even with active I-OR reactions (Figure 3). The relatively inferior cycle life in the reported 3D-disordered-structure samples may be correlated with their intrinsically limited Li de-/re-intercalated kinetics upon cycling and/or the electrode surface/interface degradation, which is briefly discussed in the supporting information and is beyond

the scope of this work. Here, we propose that the structure dimensionality can be utilized as an optimization parameter for achieving high energy density with stable I-OR in Li-rich cathode oxides. For instance, (1) the localized 3D-disordered structure dimension can be redesigned into the framework of practical Li- and Mn-rich layered oxides (with 2D-ordered structure) to improve their oxygen lattice stability; (2) a Li-rich oxide particle with gradient of structure-dimensionality could be constructed to achieve both the stable I-OR and facile Li-(de)intercalated kinetics.

In summary, the structural-dimensionality effect on the I-OR and associated oxygen lattice stability in Li-rich cathodes have been characterized and clarified. Contrasting the Li-rich TM oxides with 2D-ordered cation structure, the Li-rich TM oxides with 3D-disordered cation framework show a relatively stable oxygen lattice structure accompanying the I-OR. We explain this finding based on the different spatial-distribution of unhybridized O  $2p$  orbitals in the different structure dimensionality. This work suggests that the structure dimensionality can be designed and employed to promote the reversible I-OR with stable structure in Li-rich cathode oxides. More importantly, the findings reveal the critical structural-dimensionality effects on I-OR and its related oxygen lattice structure, paving new ways in both fundamental researches and practical developments of high-energy-density cathodes relying on stable I-OR chemistry.

## Acknowledgements

This work was supported by funding from National Key R&D Program of China (2016YFB0100100), Foundation for Innovative Research Groups of the NSFC (Grant No. 51421002), NSFC (Grant No. 11675255, 51502334, 51822211). This work used resources of the Advanced Light Source, which is a US DOE Office of Science User Facility, W.Y. acknowledges support from EERE VTO under the Applied Battery Materials Program of the US DOE, both under Contract No. DE-AC02-05CH11231.

**Keywords:** Li-ion batteries • Li-rich cathode oxides • structural dimensionality • lattice oxygen redox

- [1] a) J.-L. Shi, D.-D. Xiao, M. Ge, X. Yu, Y. Chu, X. Huang, X.-D. Zhang, Y.-X. Yin, X.-Q. Yang, Y.-G. Guo, L. Gu, L.-J. Wan, *Adv. Mater.* **2018**, *30*; b) H. Yu, H. Zhou, *J. Phys. Chem. Lett.* **2013**, *4*, 1268-1280; c) Liu, M. Hou, J. Yi, S. Guo, C. Wang, Y. Xia, *Energy Environ. Sci.* **2014**, *7*, 705-714.
- [2] a) C. Delmas, *Nature Chem.* **2016**, *8*, 641-643; b) B. Li, D. Xia, *Adv. Mater.* **2017**, *29*; c) X. Li, Y. Qiao, S. Guo, Z. Xu, H. Zhu, X. Zhang, Y. Yuan, P. He, M. Ishida, H. Zhou, *Adv. Mater.* **2018**, *30*; d) E. McCalla, A. M. Abakumov, M. Saubanere, D. Foix, E. J. Berg, G. Rousse, M.-L. Doublet, D. Gonbeau, P. Novak, G. Van Tendeloo, R. Dominko, J.-M. Tarascon, *Science* **2015**, *350*, 1516-1521.

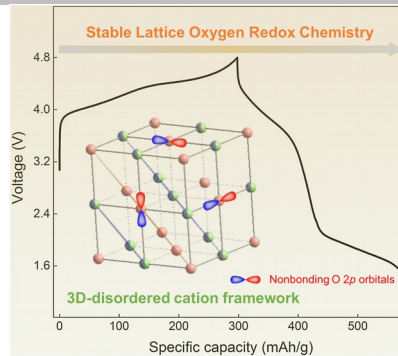
- 
- [3] a) W. Yang, *Nature Energy* **2018**, *3*, 619-620; b) E. Hu, X. Yu, R. Lin, X. Bi, J. Lu, S. Bak, K.-W. Nam, H. L. Xin, C. Jaye, D. A. Fischer, K. Amine, X.-Q. Yang, *Nature Energy* **2018**, *3*, 690-698.
- [4] D.-H. Seo, J. Lee, A. Urban, R. Malik, S. Kang, G. Ceder, *Nature Chem.* **2016**, *8*, 692-697.
- [5] R. Shunmugasundaram, R. S. Arumugam, J. R. Dahn, *J. Electrochem. Soc.* **2016**, *163*, A1394-A1400.
- [6] P. E. Pearce, A. J. Perez, G. Rousse, M. Saubanere, D. Batuk, D. Foix, E. McCalla, A. M. Abakumov, G. Van Tendeloo, M.-L. Doublet, J.-M. Tarascon, *Nature Mater.* **2017**, *16*, 580-586.
- [7] a) J. Lee, A. Urban, X. Li, D. Su, G. Hautier, G. Ceder, *Science* **2014**, *343*, 519-522.
- [8] a) W. Yang, T. P. Devereaux, *J. Power Sources* **2018**, *389*, 188-197; b) Q. Li, R. Qiao, L. A. Wray, J. Chen, Z. Zhuo, Y. Chen, S. Yan, F. Pan, Z. Hussain, W. Yang, *J. Phys. D. Appl. Phys.* **2016**, *49*, 413003.
- [9] a) N. Yabuuchi, M. Nakayama, M. Takeuchi, S. Komaba, Y. Hashimoto, T. Mukai, H. Shiiba, K. Sato, Y. Kobayashi, A. Nakao, M. Yonemura, K. Yamanaka, K. Mitsuhashi, T. Ohta, *Nat. Commun.* **2016**, *7*; b) E. Zhao, L. He, B. Wang, X. Li, J. Zhang, Y. Wu, J. Chen, S. Zhang, T. Liang, Y. Chen, X. Yu, H. Li, L. Chen, X. Huang, H. Chen, F. Wang, *Energy Storage Mater.* **2019**, *16*, 354-363.
- [10] Z. Zhuo, C. D. Pemmaraju, J. Vinson, C. Jia, B. Moritz, I. Lee, S. Sallies, Q. Li, J. Wu, K. Dai, Y. D. Chuang, Z. Hussain, F. Pan, T. P. Devereaux, W. Yang, *J. Phys. Chem. Lett.* **2018**, *9*, 6378-6384.
- [11] a) X.-D. Zhang, J.-L. Shi, J.-Y. Liang, Y.-X. Yin, J.-N. Zhang, X.-Q. Yu, Y.-G. Guo, *Adv. Mater.* **2018**, *30*; b) H. Yu, R. Ishikawa, Y.-G. So, N. Shibata, T. Kudo, H. Zhou, Y. Ikuhara, *Angew. Chem. Int. Ed.* **2013**, *52*, 5969-5973.
- [12] a) R.-P. Qiu, J.-L. Shi, D.-D. Xiao, X.-D. Zhang, Y.-X. Yin, Y.-B. Zhai, L. Gu, Y.-G. Guo, *Adv. Energy Mater.* **2016**, *6*; b) B. Qiu, M. Zhang, L. Wu, J. Wang, Y. Xia, D. Qian, H. Liu, S. Hy, Y. Chen, K. An, Y. Zhu, Z. Liu, Y. S. Meng, *Nat. Commun.* **2016**, *7*; c) B. Qiu, M. Zhang, Y. Xia, Z. Liu, Y. S. Meng, *Chem. Mater.* **2017**, *29*, 908-915.
-



## Entry for the Table of Contents

### COMMUNICATION

**Stable oxygen lattice structure** accompanying lattice oxygen redox was directly found in Li-rich cathode oxides with 3D-disordered cation framework via neutron pair distribution function and atomic-resolution scanning transmission electron microscope. The stabilization is attributed to the randomly spatial-distribution correlation among the nonbonding O 2p orbitals in this unique 3D



*Enyue Zhao<sup>+</sup>, Qinghao Li<sup>+</sup>, Fanqi Meng<sup>+</sup>, Jue Liu, Junyang Wang, Lunhua He, Zheng Jiang, Qinghua Zhang, Xiqian Yu\*, Lin Gu\*, Wanli Yang\*, Hong Li, Fangwei Wang\*, and Xuejie Huang*

**Page No. - Page No.**

**Stabilizing Oxygen Lattice and Reversible Oxygen Redox Chemistry through Structural Dimensionality in Li-rich Cathode Oxides**